Mechanism for the Compressive Strain Induced Oscillations in the Conductance of Carbon Nanotubes

L. T. Singh, S. Bhattacharyya, Abhishek K. Singh,* and K. K. Nanda†
Materials Research Centre, Indian Institute of Science, Bangalore 560012, India
(Received 13 April 2012; published 27 February 2013)

We report on the monotonic increase and the oscillation of electrical conductance in multiwalled carbon nanotubes with compressive strain. Combined experimental and theoretical analyses confirm that the conductance variation with strain is because of the transition from sp^2 to sp^3 configurations that are promoted by the interaction of walls in the nanotubes. The intrawall interaction is the reason for the monotonic increase in the conduction, while the oscillations are attributable to interwall interactions. This explains the observed electromechanical oscillation in multiwalled nanotubes and its absence in single-walled nanotubes, thereby resolving a long-standing debate on the interpretation of these results. Moreover, the current carrying capability of nanotubes can be enhanced significantly by controlling applied strains.

DOI: 10.1103/PhysRevLett.110.095504 PACS numbers: 61.48.De, 73.22.−f

The prospect of tuning the electrical conductance of carbon nanotubes (CNTs) by varying the applied mechanical strain has attracted great interest because of their potential applications in the nanoelectromechanical system [1–10]. Strain alters the band structure of a nanotube significantly and thereby, modifies the electronic transport properties. As a consequence of these effects, the current carrying capability of nanotubes can be controlled through various means including the direct growth of coiled or compressed nanotubes [11] and/or by applying strain [1–10]. These phenomena in multiwalled CNTs (MWCNTs) will introduce a myriad of possibilities for a variety of applications as electromechanical sensors, high current field effect transistors, and low resistance interconnects in electronic devices [12].

Intensive experimental and theoretical works have explored the effect of axial [1,13–15], torsional [1,16], combined axial-torsional [17,18], and radial [19] strain on the band gap of single-walled CNTs (SWCNTs). The SWCNTs exhibit a chirality dependent response to the applied strain. The zigzag and armchair SWCNTs are sensitive to axial and torsional strain [1–17], respectively, which can be used as a tool to determine the chirality of a SWCNT [20]. Strain-induced conductance change has also been observed in MWCNTs and arrays [21]. Unlike SWCNT, the conductance oscillations in MWCNT are observed only under torsional strain. Using theoretical calculations, Nagapriya *et al.* have shown that these torsion-induced conductance oscillations arise because of intrawall interactions in MWCNT [22]. The change in the band gap of the outermost wall with the torsional strain contributes to the conductance oscillations [10,22]. Here, we investigate the electrical current changes with the compressive strain on MWCNT arrays and report the electromechanical oscillation along with a monotonic increase in the conductance. This is further supported by the density functional tight binding (DFTB) calculations of the electronic band structure, exhibiting strain-induced oscillations in the band gap resulting from the change in interwall spacing under compression and an overall decrease in the band gap owing to the intrawall interaction.

The MWCNTs are synthesized by pyrolysis [23]. The mean diameter of the MWCNTs is 70 nm, and the diameter of the MWCNT arrays is 20 to 500 μm with a length of $\sim$1.0 mm. The arrays of nanotubes used in the experiments are peeled off from the quartz tube. The nanotube arrays were cyclically compressed and released along their length. The current-voltage characteristics were investigated using the Keithely 237 source measurement unit.

To investigate the electromechanical behavior of the MWCNTs, we have used an experimental setup as depicted in Fig. 1(a). The nanotubes in these arrays are held together by van der Waals forces. The MWCNT array is compressed between two electrodes, and the distance between them is controlled by rotating the screw. Scanning electron microscopy (SEM) images of the MWCNT arrays subjected to a different strain are shown in Figs. 1(b)–1(d). As a result of the compressive strain the MWCNTs get buckled only at one end as shown in Figs. 1(c) and 1(d). For this system, the compressive strain is defined as $\varepsilon = (L_0 - L)/L_0$, where L_0 is the initial length and L is the length after compression. In this setup, we were able to control the strain up to a step of 0.001, which is the smallest strain possible in our experiments. All the measurements are done at room temperature.

To understand the effect of strain on the conduction properties of the MWCNT arrays, the current-voltage (I-V) characteristics are recorded by varying the strain, i.e., by rotating the screw [Fig. 1(a)] and I-V characteristics for different ε as shown in Fig. 2(a). Similarly, current-strain (I-ε) curves are obtained at constant voltage by continuously compressing the array, and I-ε curves at different voltages are shown in the inset of Fig. 2(a).

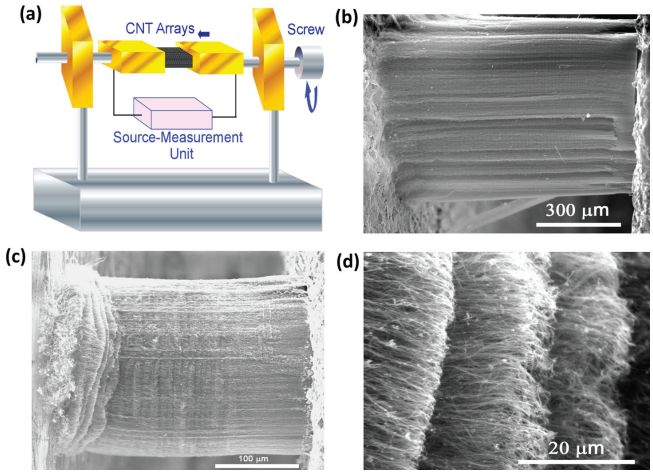

FIG. 1 (color online). (a) Schematic diagram of the experimental setup. (b) SEM image of an MWCNT array before compression. (c) SEM image of an MWCNT array after compression showing the buckling starting at one end, while the other end remains unaltered. (d) Zoomed SEM image of the buckled region.

The current increases with the compressive strain, indicating the enhancement of conductance. Most important, when the current is normalized with respect to the initial value at a particular voltage, all the I-ε curves show nearly identical qualitative and quantitative behavior as shown in Fig. 2(b). This clearly indicates a possibility of general behavior in the conductance of the MWCNTs arrays subjected to compressive strain. We fit the I-ε curves to obtain

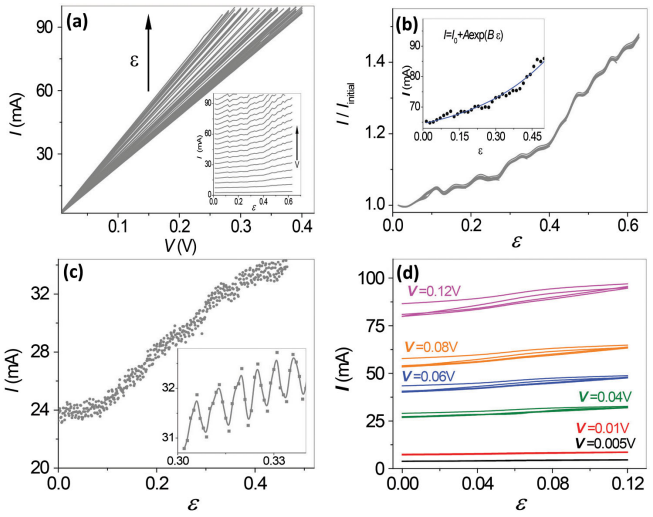

FIG. 2 (color online). (a) I-V characteristics taken at the successive compression. The bottom- and top-most curves represent the uncompressed and the most compressed arrays, respectively. Inset: I-ε at different voltages. (b) Normalized I-ε curve, where almost all the lines fall together. I-ε curve fitted with an empirical relation is shown in the inset. (c) I-ε curve measured at a step of $\varepsilon = 0.001$. A small region is extended and shown in the inset. (d) I-ε curve showing reversibility, colors of the curves represent different constant voltages.

an empirical relation, which reveals an exponential dependence $I = I_0 + A\exp(\beta\varepsilon)$ as shown in the inset of Fig. 2(b). Furthermore, the oscillations in the conductance can be seen from Fig. 2(c), which is more prominent in the zoomed region in the inset of Fig. 2(c). Current was also measured by releasing the strain, in order to observe the reversibility of the MWCNT bundle, as shown in Fig. 2(d). The plot shows excellent reversibility with a slight hysteresis at the first cycle, which disappears with the increasing number of cycles.

We further verify the experimental findings by studying the electronic structure of the MWCNT as a function of strain. The calculations were performed using the density functional based tight binding method as implemented in DFTB+ [24] code and the associated Slater-Koster parameters [25]. The system is modeled with a double-walled carbon nanotube (DWCNT), which represents the simplest MWCNT. The effect of the interwall interaction on the band gap of the individual DWCNTs under the compressive strain was studied. The atoms are allowed to relax only along the axial z direction, while constrained in the X and Y directions. In the absence of this constraint the tubes relax back to the original structure. This matches well with experiments, where tubes relax back to the original straight state once the strain is removed. The periodic boundary condition was used along the axial z direction. Sufficient vacuum (~ 15 Å) was introduced along the X and Y directions to avoid spurious interaction among the periodic images of the tubes.

We have considered five DWCNTs with chiralities $(32,0)+(23,0)$, $(44,0)+(35,0)$, $(59,0)+(50,0)$, $(71,0)+(60,0)$, and $(80,0)+(71,0)$ and denoted by DWCNT1 to DWCNT5, respectively. The choice of the chirality indices ensures that the wall-to-wall distances in DWCNT are equal to the interlayer separation of graphite. As shown in Fig. 1(d), under the compressive axial strain the MWCNT gets buckled such that the wall-to-wall distance reduces in some region and at the same time it increases in other regions. This is modeled by radial compressive strain applied to the outermost tube, keeping the inner tube unstrained, which mimics the buckled region in MWCNT under axial compression, as shown in Fig. 3(a). The strain is calculated as $\varepsilon = (r_0 - r_x)/r_0$, where r_0 is the unstrained radius and r_x is the strained radius of the outer tube along the X direction. This leads to an increase in the intrawall distance along the Y direction. As shown in Fig. 3(b), the variation of the band gap as a function of the applied strain exhibits electromechanical oscillations. For smaller strain the decrease in band gap is minimal as the wall-to-wall distances are still not sufficient to invoke covalent interactions. After a threshold value of strain (ε_{th}) the band gap falls sharply and exhibits the electromechanical oscillations. The threshold strain decreases with an increase in diameter of the DWCNT. The corresponding wall-to-wall distance at which the oscillations were

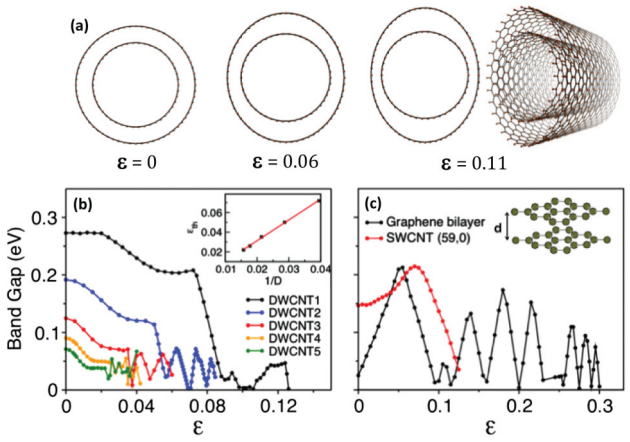

FIG. 3 (color online). (a) The supercell of one of the DWCNTs under different strain conditions. Cross-sectional view of DWCNT1 (diameter of 25.37 Å) under various $\varepsilon = 0.0$, 0.6, and 0.11. The side view of the structure with $\varepsilon = 0.11$ is also shown. (b) Change in band gap as a function of radial strain for DWCNT1 to DWCNT5. Inset: Threshold strain after which oscillation starts as a function of diameter inverse of the DWCNTs. (c) Similar to (b), for SWCNT of diameter 46.78 Å and band gap variation of a bilayer *AA* stacked graphene as a function of vertical strain. Inset: Atomic structure of *AA* stacked bilayer graphene. The band structures are calculated on a $1 \times 1 \times 20$ K-grid.

observed is invariant for all the tubes and represents the distance at which the covalent interactions between two tubes start. Therefore, for larger DWCNTs this critical separation is achieved at comparatively lower strains. The plot [Fig. 3(b), inset] of ε_{th} as a function of the inverse of the DWCNT diameter shows a linear dependence. From the extrapolation of the graph, we see that ε_{th} goes to zero for the tube diameter of ~20 nm. This means that the plateau region (the region before the oscillation starts) will be absent for tubes having a larger diameter. Also, the fact that oscillations were observed for larger tubes starting at lower strain brings the results closer to the experimental observations. Therefore, with an increasing diameter we would be able to achieve a better agreement with the experiments. Finally, for the asymptotic limit of an infinite diameter nanotube, i.e., graphene, the oscillations start at an infinitesimally small strain [Fig. 3(c)]. Furthermore, the overall band gap increases with a decreasing diameter [Fig. 3(b)] because of quantum confinement, which has also been observed experimentally for SWCNTS [26,27]. Therefore, the larger diameter tubes will have an even smaller gap, resulting in the smaller oscillation in the conductance, which will have a better agreement with the experiments.

To separate the effects of intra- and interwall interactions on the electromechanical properties of MWCNT, we have calculated the band gap of the freestanding outer tube (59, 0) subjected to the same radial strain. Similar to the case of MWCNTs, the change in the band gap with strain [Fig. 3(c)] shows a broad peak near a strain of 0.07 followed by a monotonic decrease of the band gap. However, unlike MWCNTs, there is a complete absence of electromechanical oscillation. The effect of the interwall interaction on electromechanical properties was evaluated by calculating the band structure of the *AA* stacked bilayer graphene as a function of interlayer distances. The *AA* stacking of graphene layers resembles the region where the layers of the inner and the outer tubes come closer under radial compression as shown in the inset of Fig. 3(c). The initial interlayer distance of the *AA* graphene was equal to the interwall distance of the DWCNTs. Similar to the DWCNTs, the band gap of the bilayer *AA* graphene structure shows strong oscillations with an increasing strain [Fig. 3(c)]. These oscillations are not regular and can be explained based on the zone folding scheme for graphene. In a DWCNT, the two overlapping Brillouin zones continuously change with an application of strain thereby changing the band structure itself. Whenever the high symmetric "K point" is included in the Brillouin zone, a dip in the band gap versus the strain curve is observed, which is very irregular because of the lack of a fixed relationship between the chiralities of the tubes involved. To investigate this, we further calculated analytically the electronic structure of the strained *AA* graphene bilayer by deriving a tight binding Hamiltonian, where a correction term was added to describe the normal strain. The value of the hopping parameter between the nearest neighbor carbon atoms of the two different layers was rescaled for each strain using various approaches [28–30]. Similar irregular oscillations [as in Fig. 3(c)] were again obtained analytically (details will be published elsewhere) for bilayer graphene as well. Therefore, inter- and intrawall interactions lead to the electromechanical oscillation and monotonic decrease in the band gap, respectively. The combined effect is similar to the behavior observed in the experiments as shown in Fig. 3(b). Indeed, in the experimental setup, a bundle of MWCNTs consists of tubes with various chiralities, which leads to different quantitative results owing to an averaging effect, yet the overall qualitative behavior remains unchanged as shown in Figs. 2(b) and 2(c).

Next, we analyze the origin of the respective highest occupied molecular orbital and lowest unoccupied molecular orbital of DWCNT2 under different strains. These states arise from the interwall interaction as shown in Figs. 4(a)–4(d). The intertube interactions are very prominent in the regions, where the distance is minimum, showing strong evidence of sp^2 to sp^3 transition. On the other hand, the regions where the walls are furthest, do not contribute to these states. Therefore, the electromechanical oscillations are indeed originating from the tube-tube interactions in the closer region, which is eventually caused by the sp^2 to sp^3 transition.

We further characterized the compressed MWCNTs arrays by Raman spectroscopy to substantiate the evident transition from sp^2 to sp^3 as predicted by DFTB

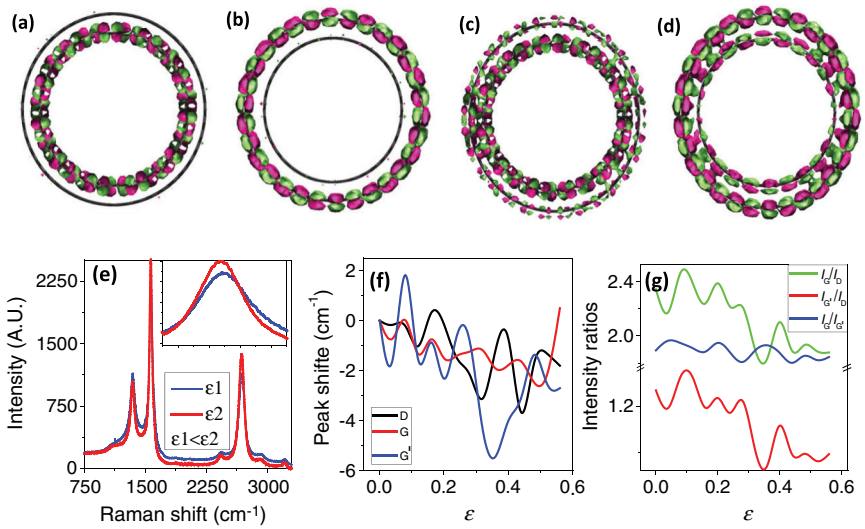

FIG. 4 (color online). (a) Highest occupied molecular orbital and (b) lowest unoccupied molecular orbital wave function (green for positive and magenta for negative) of unstrained DWCNT2 (diameter of 34.89 Å). (c) and (d) show similar plots for the same DWCNT under a strain of 0.03. Isovalue was taken as 0.002 for all the plots. (e) Raman spectra with two different compressive strains. Inset shows the relative shifts in the peak position. (f) Relative peak positions. (g) Intensity ratios of G to D (green curve), G' to D (red curve), and G to G' (blue curve) with strain.

calculations. The Raman spectra of carbon nanotube arrays for two different compressive strains are shown in Fig. 4(e). The inset of Fig. 4(e) reveals the shift of the G peak with strain. Figures 4(f) and 4(g) show the shifting of the relative peak positions and the variation of intensity ratios (I_G/I_D, $I_{G'}/I_D$, and $I_G/I_{G'}$) with the strain, respectively. The intensity ratios and the position of the Raman peaks vary in a similar fashion, as is the case of conductance. While the oscillatory nature is because of the sp^2 to sp^3 transition caused by the interwall interaction, the overall frequency decrease is because of the increase of the C-C bond length [31,32]. From the intensity ratios, we see the disorder-induced peak (D peak) is becoming more prominent with the increase of the strain. This indicates that the transition of sp^2 to sp^3 is prevailing when the arrays are subjected to compressive strain. It has been shown that the sp^2 to sp^3 transition is possible for MWCNTs, especially when the interwall separation decreases [33]. Our combined experimental and theoretical results also suggest that the sp^2 to sp^3 transition is because of the interwall interaction. Over all, we observe the oscillatory nature of the peak positions and intensity ratios, which are related to the oscillation in polarizability caused by induced disorder.

The other possibility that may influence the conductance is the formation of defects. In nanotubes, the defect formation energies are quite high, which implies that their concentration is going to be very low. Furthermore, with applied strain, the conductance shows the oscillatory behavior with an overall increase, while a slight decrease is found after the completion of the first cycle [Fig. 2(d)]. The overall trend remains same after several cycles. Therefore, the increase in conductance is very unlikely to be caused by the formation of defects.

We report on the monotonic increase and the oscillation of conductance in MWCNTs with compressive strain. The intrawall interaction is the reason for the monotonic increase in the conduction, while the interaction of different walls in MWCNT promotes sp^2 to sp^3 configurations leading to the oscillations in the conductance. This resolves the long-standing debate on the observed electromechanical oscillations in MWCNT and their absence in SWCNT. The current carrying capability of MWCNTs can be enhanced significantly by controlling applied strains and/or direct growth of coiled or compressed nanotubes. Most important, this can be achieved reversibly, leading to the possibility of designing electromechanical sensors, high current field effect transistors, and low resistance interconnects in electronic devices.

The authors acknowledge Professor P. M. Ajayan and Professor P. Jena for useful discussions. The authors also acknowledge financial support from ADA under NPMASS. We thankfully acknowledge the Supercomputer Education and Research Centre, Indian Institute of Science for its computing facilities. L. T. Singh and S. Bhattacharyya contributed equally to this work.

*Corresponding author.
abhishek@mrc.iisc.ernet.in
†Corresponding author.
nanda@mrc.iisc.ernet.in

[1] L. Yang and J. Han, Phys. Rev. Lett. **85**, 154 (2000).
[2] S. Paulson, M. R. Falvo, N. Snider, A. Helser, T. Hudson, A. Seeger, R. M. Taylor, R. Superfine, and S. Washburn, Appl. Phys. Lett. **75**, 2936 (1999).

[3] T. W. Tombler, C. Zhou, L. Alexseyev, J. Kong, H. Dai, L. Liu, C. S. Jayanthi, M. Tang, and S.-Y. Wu, Nature (London) **405**, 769 (2000).
[4] E. D. Minot, Y. Yaish, V. Sazonova, J.-Y. Park, M. Brink, and P. L. McEuen, Phys. Rev. Lett. **90**, 156401 (2003).
[5] J. Cao, Q. Wang, and H. Dai, Phys. Rev. Lett. **90**, 157601 (2003).
[6] C. Stampfer, A. Jungen, R. Linderman, D. Obergfell, S. Roth, and C. Hierold, Nano Lett. **6**, 1449 (2006).
[7] L. Liu, C. S. Jayanthi, M. Tang, S. Y. Wu, T. W. Tombler, C. Zhou, L. Alexseyev, J. Kong, and H. Dai, Phys. Rev. Lett. **84**, 4950 (2000).
[8] A. Maiti, A. Svizhenko, and M. P. Anantram, Phys. Rev. Lett. **88**, 126805 (2002).
[9] T. Cohen-Karni, L. Segev, O. Srur-Lavi, S. R. Cohen, and E. Joselevich, Nat. Nanotechnol. **1**, 36 (2006).
[10] A. R. Hall, M. R. Falvo, R. Superfine, and S. Washburn, Nat. Nanotechnol. **2**, 413 (2007).
[11] P. Castrucci, M. Scarselli, M. De Crescenzi, M. A. El Khakani, F. Rosei, N. Braidy, and J. H. Yi, Appl. Phys. Lett. **85**, 3857 (2004).
[12] S. J. Kang, C. Kocabas, T. Ozel, M. Shim, N. Pimparkar, M. A. Alam, S. V. Rotkin, and J. A. Rogers, Nat. Nanotechnol. **2**, 230 (2007).
[13] L.-J. Pan, Y. Jia, Q. Sun, and X. Hu, Chin. Phys. Lett. **28**, 087103 (2011).
[14] S. Ogata and Y. Shibutani, Phys. Rev. B **68**, 165409 (2003).
[15] P. K. Valavala, D. Banyai, M. Seel, and R. Pati, Phys. Rev. B **78**, 235430 (2008).
[16] S.-M. Choi and S.-H. Jhi, Carbon **46**, 773 (2008).
[17] S. Wang, R. Wang, X. Wu, H. Zhang, and R. Liu, Physica (Amsterdam) **42**, 2250 (2010).
[18] Y. Zhang and M. Han, Physica (Amsterdam) **43**, 1774 (2011).
[19] Y. V. Shtogun and L. M. Woods, Carbon **47**, 3252 (2009).
[20] L.-J. Li, R. J. Nicholas, R. S. Deacon, and P. A. Shields, Phys. Rev. Lett. **93**, 156104 (2004).
[21] J. Suhr, P. Victor, L. Ci, S. Sreekala, X. Zhang, O. Nalamasu, and P. M. Ajayan, Nat. Nanotechnol. **2**, 417 (2007).
[22] K. S. Nagapriya, S. Berber, T. Cohen-Karni, L. Segev, O. Srur-Lavi, D. Tománek, and E. Joselevich, Phys. Rev. B **78**, 165417 (2008).
[23] P. Mahanandia and K. K. Nanda, Nanotechnology **19**, 155602 (2008).
[24] B. Aradi, B. Hourahine, and T. Frauenheim, J. Phys. Chem. A **111**, 5678 (2007).
[25] C. Köhler and T. Frauenheim, Surf. Sci. **600**, 453 (2006).
[26] T. W. Odom, J.-L. Huang, P. Kim, and C. M. Lieber, Nature (London) **391**, 62 (1998).
[27] J. W. G. Wildöer, L. C. Venema, A. G. Rinzler, R. E. Smalley, and C. Dekker, Nature (London) **391**, 59 (1998).
[28] W. A. Harrison, *Elementary Electronic Structure* (World Scientific, Singapore, 1999).
[29] D. A. Papaconstantopoulos, M. J. Mehl, S. C. Erwin, and M. R. Pederson, *Tight-Binding Approach to Computational Materials Science*, edited by P. Turchi, A. Gonis, and L. Colombo (Materials Research Society, Pittsburgh, 1998), p. 221.
[30] V. M. Pereira, A. H. Castro Neto, and N. M. R. Peres, Phys. Rev. B **80**, 045401 (2009).
[31] S. B. Cronin, A. K. Swan, M. S. Ünlü, B. B. Goldberg, M. S. Dresselhaus, and M. Tinkham, Phys. Rev. Lett. **93**, 167401 (2004).
[32] S. B. Cronin, A. K. Swan, M. S. Ünlü, B. B. Goldberg, M. S. Dresselhaus, and M. Tinkham, Phys. Rev. B **72**, 035425 (2005).
[33] W. Guo, C. Z. Zhu, T. X. Yu, C. H. Woo, B. Zhang, and Y. T. Dai, Phys. Rev. Lett. **93**, 245502 (2004).